

Instrumentation for and First Results on Nuclear Responses for Supernova Explosions

H.J. Wörtche^a *

for the EUROSUPERNOVA collaboration**

^aInstitut für Kernphysik, Westfälische Wilhelms-Universität,
Wilhelm-Klemm-Strasse 9, 48149 Münster, Germany

Our collaboration has set up a focal plane detection system and a focal plane polarimeter at the large acceptance Big-Bite Spectrometer at AGOR. The detector systems are equipped with a high performance readout and online data processing system, which allows polarization transfer and charge transfer measurements at extreme forward angles with high precision. Preliminary results on GT_+ strength distributions obtained in $(d, ^2\text{He})$ measurements revealing the fine structure of the distributions are presented. Their relation to recent calculations of stellar weak interaction rates is discussed.

1. Introduction

In the past years great efforts have been made to improve the reliability of theoretical predictions used to calculate stellar weak interaction rates. Special emphasis has been put on allowed and first-forbidden Gamow-Teller (GT) and Fermi (F) transitions, which govern electron-capture, positron-capture and β -decay rates, as well as ν -nucleosynthesis in different stages of a supernova event. To obtain predictions with significantly improved reliability, as compared to the standard work performed by Fuller, Fowler and Newman [1–4], rates have recently been determined based on systematic large-scale shell model calculations in the mass range $A = 45\text{--}65$ [5,6]. The reliability of the calculations has been tested by comparing the excitation spectra as well as the GT_- and GT_+ strength distributions with experimental data. In case of the GT strengths, the crucial condition was a proper reproduction of the GT strength distributions deduced from (p, n) and (n, p) measurements and emphasis was put on transitions leading to the population of low-lying states, where due to phase space enhancement the (fine) structure of the distributions gets relevant [5].

With this theoretical tool available, experiments are needed, which provide information on GT strength distributions with improved precision, compared to the pioneering (p, n) and (n, p) experiments (for the nuclei of consideration see [5] and references therein). A successful experimental approach has been demonstrated in Refs. [7,8]. A combined analysis of high resolution $(^3\text{He}, t)$, (p, p') and (e, e') data yielded information on the

*Present address: Kernfysisch Versneller Instituut, Rijksuniversiteit Groningen, Groningen, The Netherlands, E-mail : wortche@kvi.nl

structure of the GT strength distribution and the separation of isospin components in ^{28}Si and ^{58}Cu .

Following the approach of combining the spin-isospin selectivity of hadronic probes, the EUROSUPERNOVA collaboration has set up and commissioned a focal plane detection system (FPDS) and a high performance focal plane polarimeter (FPP) at the large acceptance Big-Bite Spectrometer (BBS) [9] at AGOR. Taking advantage of various particle beams provided at medium energies ($E/A \simeq 100 - 200$ MeV) by the AGOR cyclotron, the system is bound to perform polarization transfer measurements in inelastic proton scattering and charge exchange reactions like $(d, {}^2\text{He})$ and $({}^3\text{He}, t)$. The experiments are performed at extreme forward angles, including 0° , where due to the momentum dependence of the hadronic interaction the scattering becomes especially sensitive for excitation of spin-flip transitions.

In section 2 of this contribution, we present a short overview of the detector setup, the detector readout and the Digital Signal Processor (DSP) based data acquisition system. In section 3, preliminary experimental results are presented. For details of the setup we refer to Refs. [10–12].

2. The EUROSUPERNOVA detector system

2.1. Detector setup

In Fig.1 a schematic layout of the EUROSUPERNOVA detector is depicted. In order to deduce the momentum vector, scattered particles are detected near the BBS focal plane using a set of Vertical Drift Chambers (VDC's) VDC1 and VDC2. The momentum acceptance of the system with the BBS in mode B is about 15%. The angular acceptance is 66 mrad in the horizontal and 140 mrad in the vertical direction. The energy resolution achieved for 150 MeV protons is 100 keV FWHM.

If the detector is operated in polarimeter mode, the polarization of scattered particles is deduced by measuring the asymmetry of 2^{nd} scattering in the graphite analyzer C. Tracking upstream and downstream of the analyzer is performed by virtue of a set of Multi Wire Proportional Chambers (MWPC's) D1 - D4. The angular acceptance for 2^{nd} scattering is limited to angles smaller than 20° .

2.2. Detector readout

Operation at extreme forward angles causes high rate loads in the detection system. In addition, the rates in different sections of the wire chambers may differ as much as 5 orders of magnitude. To guarantee a flat efficiency, the wire chambers have been equipped with newly developed ASD-8 based preamplifiers, which are capable of processing data up to 30 MHz without significant pile-up [12]. The preamplifiers provide differential low-swing ECL signals, which are transferred via ECL level converters to the CAMAC based front-end electronics (see Fig.2). The integrated charge information is maintained in the width of the signals, a feature which might allow energy-resolving detection in future applications. The MWPC data are processed by the LeCroy PCOS III system, the VDC data by the LeCroy pipeline TDC system 3377 [13]. Readout of the complete detector, in total about 4000 wires, is accomplished in less than $7 \mu\text{s}$ for a standard event.

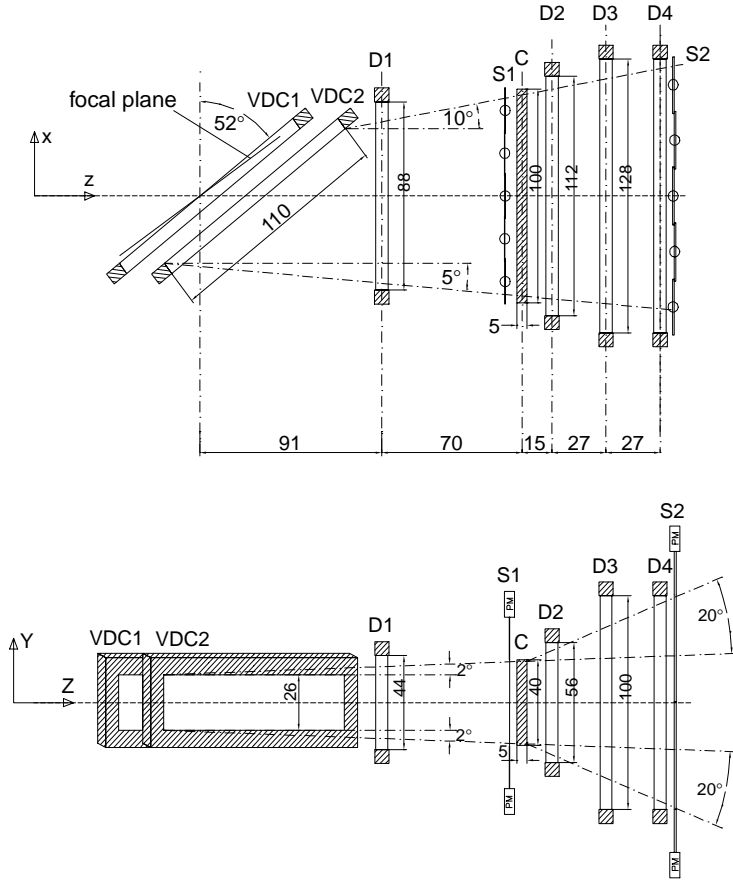


Figure 1. Top view (upper panel) and side view (lower panel) of the EUROSUPERNOVA detector. The FPDS consists of two VDC's, tilted 52° to the normal of the central beam. Tracking in the FPP is performed by four MWPC's D1 - D4. Two segmented scintillator arrays are labelled as S1 and S2, the graphite analyzer is labelled as C. Lengths are indicated in units of centimeters. (Figure adapted from Ref. [11]).

2.3. Data acquisition and online processing

In inelastic proton scattering, a major constraint performing polarization transfer measurements is the by far dominant small-angle Coulomb scattering in the analyzer. This effect limits the angular range, where usable asymmetries can be obtained to angles larger than 5° and reduces the polarimeter efficiency to about 5 %.

In the present setup, a DSP based data acquisition system has been implemented, which performs a readout of *each* event triggered by a coincidence of scintillator planes S1 and S2 and subsequently performs a software evaluation of the data. This solution offers great flexibility. Changing the detector e.g. from (\vec{p}, \vec{p}') -mode to $(d, ^2\text{He})$ -mode, described below, solely requires reprogramming of the DSP's and removal of the graphite analyzer. Also operating the detector in coincidence to other detector systems is greatly simplified and can be achieved through synchronization to the 1st level trigger, as has

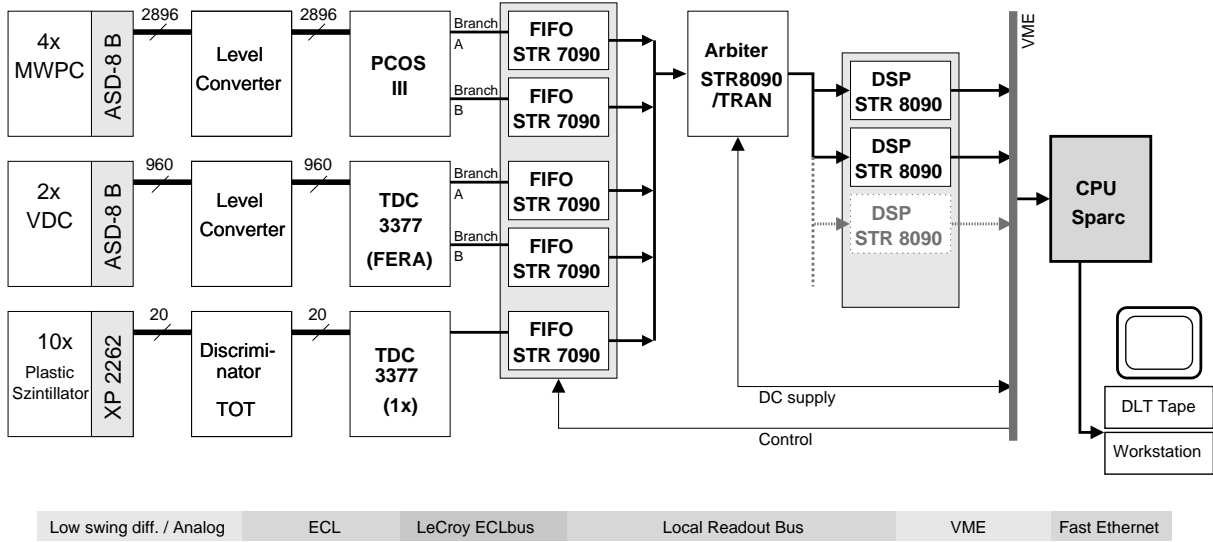


Figure 2. Scheme of the DSP-based data acquisition system. The amount of active channels, sense wires for wire chambers, photomultipliers for scintillator arrays, are indicated. (Figure adapted from Ref. [11]).

been successfully tested for the $^{26}\text{Mg}(^3\text{He}, t\gamma)^{26}\text{Al}^*$ reaction [14].

Maximum performance is achieved by matching the processing and the readout time and decoupling the DSP's from the random front-end data by a FIFO system. The present setup is capable of handling an incoming rate up to several hundred kHz, with the DSP not contributing to the system dead time [11].

3. Preliminary experimental results

After commissioning the setup, our collaboration has performed high statistics cross section and polarization transfer measurements of inelastic proton scattering from ^{11}B , ^{12}C , ^{48}Ca , ^{58}Ni and ^{124}Sn . The experiments are mainly geared to extract spin-flip M1 and spin-dipole strengths distributions up to 30 MeV excitation, the data are presently analyzed.

In addition, we have started to investigate the GT_+ strength distribution in a $A=45\text{-}65$ mass nucleus via the reaction $^{58}\text{Ni}(d, ^2\text{He})^{58}\text{Co}$ and supplementary calibration measurements $^{12}\text{C}(d, ^2\text{He})^{12}\text{B}$ and $^{24}\text{Mg}(d, ^2\text{He})^{24}\text{Na}$ at scattering angles $\theta = 0^\circ - 27^\circ$.

The performance of $(d, ^2\text{He})$ measurements at extreme forward angles including 0° is a non trivial exercise, because it requires coincident detection of correlated proton pairs originating from the unbound ^2He -system in the vicinity of a dominant background caused by deuteron breakup protons. In order to operate the EUROSUPERNOVA detector in $(d, ^2\text{He})$ -mode, the graphite analyzer is removed and the DSP's are reprogrammed to identify tracks of correlated protons by means of the MWPC information. Due to the limited angular acceptance of the BBS, detected ^2He proton pairs originate from the target

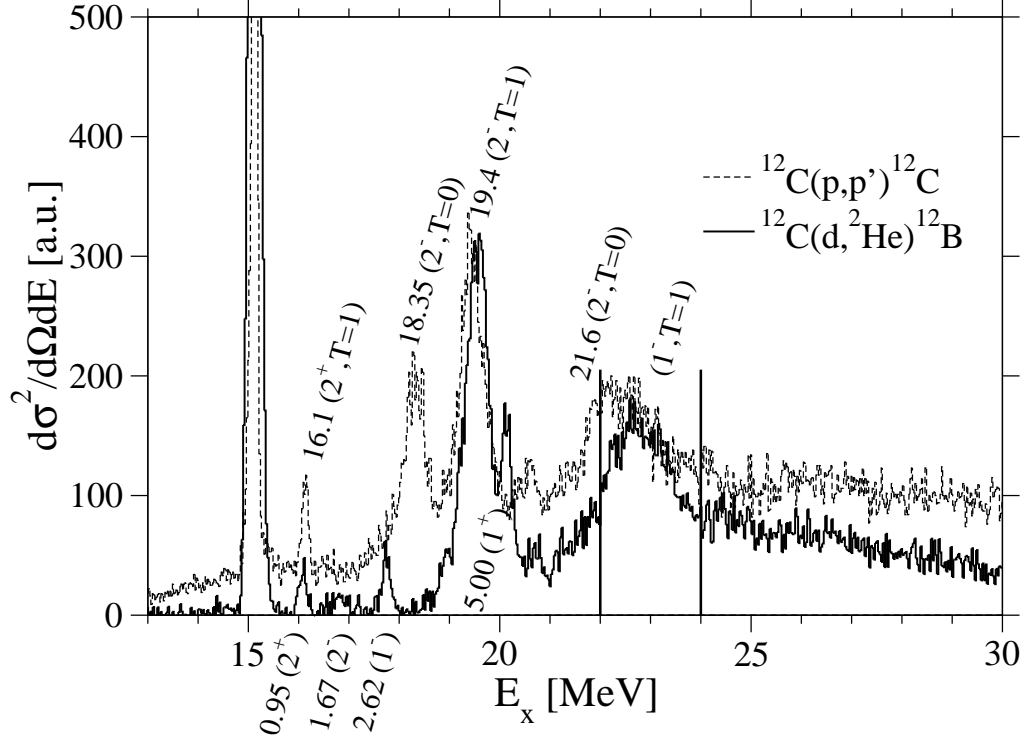


Figure 3. Double differential $^{12}\text{C}(p,p')^{12}\text{C}$ and $^{12}\text{C}(d,^2\text{He})^{12}\text{B}$ cross section spectra measured for $E_p=172$ MeV, $\theta = 10^\circ$ and for $E_d=170$ MeV, $\theta = 0^\circ$, respectively. The $(d,^2\text{He})$ cross sections are not acceptance corrected and are shifted by 15.11 MeV (see text). Prominent excitations in ^{12}C [15] are indicated above, prominent excitations in ^{12}B [15] below the spectra. The latter excitation energies refer to the ^{12}B ground state. The vertical lines mark a range of ^{12}C ($J^\pi, T = 1^-, 1$) excitations.

with small (relative) kinetic energy, i.e. the ^2He system is nearly exclusively detected in 1S_0 configuration. The $(d,^2\text{He})$ reaction therefore acts as a filter for $\Delta S = \Delta T = 1$ transitions, if a simple one-step reaction mechanism is assumed.

Figure 3 shows a $^{12}\text{C}(d,^2\text{He})^{12}\text{B}$ double-differential cross section spectrum measured at 0° and $E_d=170$ MeV with a (p,p') double-differential cross section spectrum measured at 10° and $E_p=172$ MeV overlaid. The data taking time for the $(d,^2\text{He})$ spectrum amounted to 4 hours. The transition to the ^{12}B ground-state and the analogue 15.11 MeV spin-flip M1 transition in ^{12}C have been matched in energy by shifting the $(d,^2\text{He})$ spectrum by 15.11 MeV.

The energy resolution achieved for excitations in the residual nucleus ^{12}B is about 150 keV, revealing the fine structure of the ^{12}B spin-isospin response. The spectrum is free from background originating from random coincidence breakup protons. Both features could be achieved by applying a novel VDC analysis method based on imaging techniques during offline analysis [16]. The software is capable of identifying multiple tracks in the VDC's based on the pipeline TDC event history, even in case of spatial overlap, and

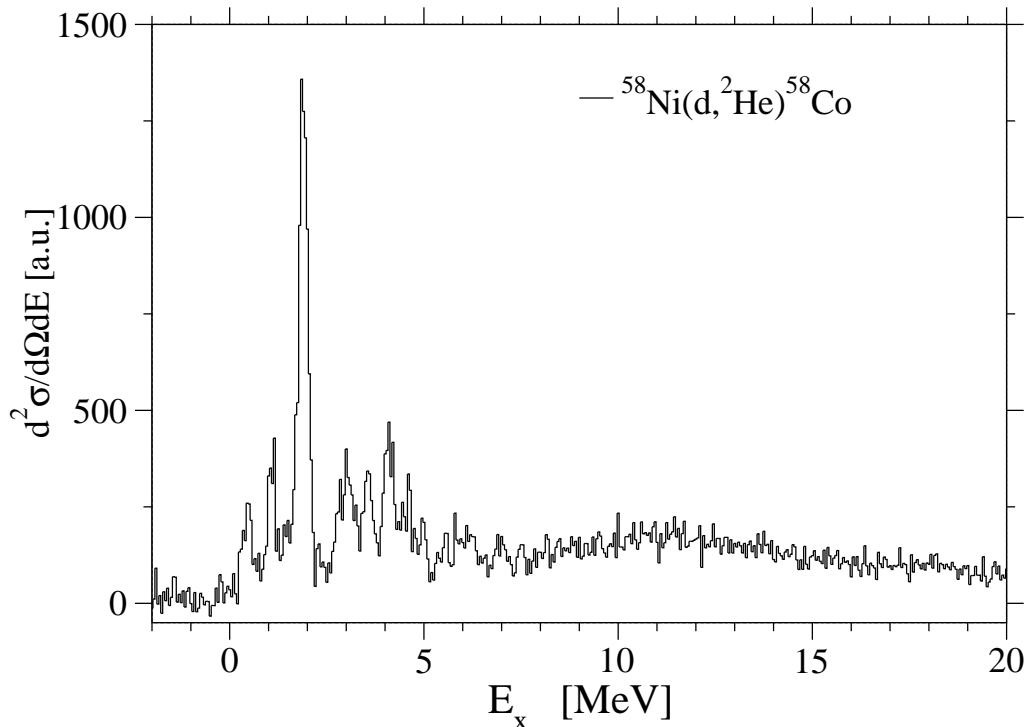


Figure 4. Double differential $^{58}\text{Ni}(d,^2\text{He})^{58}\text{Co}$ cross section spectrum. Excitation energies refer to the ^{58}Co ground-state. The cross sections are acceptance corrected.

provides the time difference of particles passing the VDC wire-planes. Based on the later information, the shape of the random background is identified by correlating protons stemming from different beam bursts in the analysis.

The comparison illustrated in Fig.3 demonstrates, similar as in earlier measurements [17–19], the selectivity of the $(d,^2\text{He})$ probe for the excitation of spin-isospin modes. The energy resolution we obtain nevertheless removes systematic uncertainties in identifying analogue transitions, one of the major obstacles encountered in identifying GT_+ strengths distributions in the past.

In Fig.4, we present a 0° $(d,^2\text{He})$ cross section spectrum measured at $E_d=170$ MeV for ^{58}Ni , a nucleus in the mass range under consideration in Refs.[5,6]. The spectrum is acceptance corrected, by modeling the BBS ^2He acceptance in Monte-Carlo simulations. Up to 5 MeV excitation in ^{58}Co , we detect a concentration of transitions, most prominent a strong transition at about 1.9 MeV. The transitions correlate to the broad distribution of GT_+ strength detected in (n, p) measurements [20] and the analogue $T_0 + 1$ strength distribution deduced from $^{58}\text{Ni}(^3\text{He}, t)^{58}\text{Cu}$ data [7]. Relating to the issue of the relative importance of low-lying transitions mentioned above, our data indicate distinct differences in the GT_+ strength distribution below 5 MeV compared to the earlier measurements, an

issue which will be subject of further investigations and requires careful consideration of the physics underlying the different probes.

At higher excitations the ($d, ^2\text{He}$) cross section spectra reveal the existence of a brought resonant structure centered at about 11 MeV, which becomes most prominent at a scattering angle of 3° . The observed resonance coincides with the spin-dipole strength distribution obtained in a multipole analysis of $^{58}\text{Ni}(n, p)^{58}\text{Co}$ cross sections [20].

4. Acknowledgements

This work was supported by the European Union through the Human Capital and Mobility Program under contract number ERB4050PL932447 and the Large-Scale Facility program LIFE under contract number ERBFMGECT980125 and the Land Nordrhein-Westfalen. It was performed as part of the research program of the Fund for Scientific Research (FSR) Flanders and the Stichting voor Fundamenteel Onderzoek der Materie (FOM) with financial support from the Nederlandse Organisatie voor Wetenschappelijk Onderzoek (NWO).

**The EUROSUPERNOVA collaboration

R. Bassini^{f)}, C. Bäumer^{a)}, F. Bauwens^{b)}, A.M. van den Berg^{g)}, N. Blasi^{f)}, C. De Coster^{b)}, A.E.L. Dieperink^{g)}, F. Ellinghaus^{a)}, D. Frekers^{a)}, D. De Frenne^{b)}, M. Hagemann^{b)}, V.M. Hannen^{g)}, M.N. Harakeh^{g)}, R. Hendersonⁱ⁾, K. Heyde^{b)}, J. Heyse^{b)}, M.A. de Huu^{g)}, E. Jacobs^{b)}, B.A.M. Krüsemann^{g)}, K. Langanke^{h)}, R. De Leo^{e)}, M. Malatesta^{f)}, S. Micheletti^{f)}, M. Mielke^{a)}, P. von Neumann-Cosel^{c)}, M. Pignanelli^{f)}, S. Rakers^{a)}, B. Reitz^{c)}, A. Richter^{c)}, R. Schmidt^{a)}, G. Schrieder^{c)}, H. Sohlbach^{d)}, A. Stascheck^{c)}, S.Y. van der Werf^{g)}, H. De Witte^{b)}, H.J. Wörtche^{a)}

a) Westfälische Wilhelms-Universität, Münster, Germany

b) Universiteit Gent, Gent, Belgium

c) TU Darmstadt, Darmstadt, Germany

d) Märkische Fachhochschule, Iserlohn, Germany

e) Università degli Studi Bari, Bari, Italy

f) INFN, Milano, Italy

g) Kernfysisch Versneller Instituut, Groningen, The Netherlands

h) Aarhus Universitet, Aarhus, Denmark

i) TRIUMF, Vancouver, Canada

REFERENCES

1. G. Fuller, W. Fowler, M. Newman, ApJS 42 (1980) 447.
2. G. Fuller, W. Fowler, M. Newman, ApJS 48 (1982) 279.
3. G. Fuller, W. Fowler, M. Newman, ApJ 252 (1982) 715.
4. G. Fuller, W. Fowler, M. Newman, ApJ 293 (1985) 1.
5. E. Caurier, K. Langanke, G. Martínez-Pinedo, F. Nowacki, Nucl. Phys. A 653 (1999) 439.
6. K. Langanke, G. Martínez-Pinedo, Nucl. Phys. A 673 (2000) 481.
7. Y. Fujita, H. Akimune, I. Daito, M. Fujiwara, M. Harakeh, T. Inomata, J. Jänecke,

- K. Katori, H. Nakada, S. Nakayama, A. Tamii, M. Tanaka, H. Toyokawa, M. Yosoi, Phys. Lett. B 365 (1996) 29.
8. Y. Fujita, H. Akimune, I. Daito, M. Fujiwara, M. Harakeh, T. Inomata, J. Jänecke, K. Katori, C. Lüttge, S. Nakayama, P. von Neumann-Cosel, A. Richter, A. Tamii, M. Tanaka, T. H. U. a. M. Yosoi, Phys. Rev. C 55 (1997) 1137.
 9. A. van den Berg, Nucl. Instr. and Meth. B 99 (1995) 637.
 10. B. Krüsemann, R. Bassini, F. Ellinghaus, D. Frekers, M. Hagemann, V. Hannen, H. von Heynitz, J. Heyse, S. Rakers, H. Sohlbach, H. Wörtche, Nucl. Instr. Meth. A 431 (1999) 236.
 11. M. Hagemann, R. Bassini, A. van den Berg, F. Ellinghaus, D. Frekers, V. Hannen, T. Häupkea, J. Heyse, E. Jacobs, M. Kirsch, B. Krüsemann, S. Rakers, H. Sohlbach, H. Wörtche, Nucl. Instr. and Meth. A 437 (1999) 459.
 12. B. Krüsemann, R. Bassini, C. Bäumer, A. van den Berg, N. Dresnandt, D. Frekers, M. Hagemann, V. Hannen, R. Henderson, , J. Heyse, M. de Huu, M. Newcomer, S. Rakers, B. Reitz, R. Schmidt, H. Sohlbach, H. Wörtche, IEEE Trans. Nucl. Sci., submitted for publication .
 13. LeCroy Corp. Internet page, <http://www.lecroy.com/lsr/>.
 14. S. Sakoda, A. van den Berg, N. Blasi, F. Camera, F. Ellinghaus, D. Frekers, M. Greenfield, M. Hagemann, V. Hannen, M. Harakeh, M. Hatano, J. Heyse, M. de Huu, B. Krüsemann, Y. Maeda, T. Ohnishi, S. Rakers, H. Sakai, A. Tamii, T. Uesaka, H. Wörtche, K. Yako, R. Zegers, KVI Annual Report (1999) 3.
 15. F. Ajzenberg-Selove, Nucl. Phys. A 506 (1990) 1.
 16. R. Schmidt, Diploma thesis, Westfälische Wilhelms-Universität Münster, Institut für Kernphysik .
 17. H. Ohnuma, K. Hatanaka, S. Hayakawa, M. Hosaka, T. Ichihara, S. Ishida, S. Kato, T. Niizeki, M. Ohura, H. Okamura, H. Orihara, H. Sakai, H. Shimizu, Y. Tajima, H. Toyokawa, H. Yoshida, M. Yosoi, Phys. Rev. C 47 (1993) 648.
 18. H. Xu, G. Ajupova, A. Betker, C. Gagliardi, Y. L. B. Kokenge, A. Zaruba, Phys. Rev. C 52 (1995) R1161.
 19. T. Inomata, H. Akimune, I. Daito, H. Ejiri, H. Fujimura, Y. Fujita, M. Fujiwara, M. Harakeh, K. Ishibashi, H. Kohri, N. Matsuoka, S. Nakayama, A. Tamii, M. Tanaka, H. Toyokawa, M. Yoshimura, M. Yosoi, Phys. Rev. C 57 (1998) 3153.
 20. S. El-Kateb, K. Jackson, W. Alford, R. Abegg, R. Azuma, B. Brown, A. Celler, D. Frekers, O. Häusser, R. Helmer, R. Henderson, K. Hicks, J. K. R. Jeppesen, K. Raywood, G. Shute, B. Spicer, A. Trudel, M. Vetterli, S. Yen, Phys. Rev. C 49 (1994) 3128.